

Resonant structure in electron impact excitation of CO near threshold

N. Swanson, R. J. Celotta, C. E. Kuyatt, and J. W. Cooper

National Bureau of Standards, Washington, D.C. 20234

(Received 7 February 1975)

Electron impact excitation functions of numerous states in CO have been measured at 45° scattering angle with resolutions of 16–23 meV FWHM. The decay peak of the 10.04 eV resonance can be seen in the results for the $a^3\Pi$, $a'^3\Sigma^+$, and $A^1\Pi$ vibrational levels. There was no evidence of resonant excitation of the $a'^3\Sigma^+$ state near 8 eV as suggested by Newton and Thomas. Excitation functions of the $b^3\Sigma^+$, $B^1\Sigma^+$, $C^1\Sigma^+$, $c^3\Pi$, and $E^1\Pi$ states, and a previously unobserved state at 11.26 eV show numerous sharp resonances in the first few eV above threshold. Energy loss spectra in the 8–14 eV loss region show peaks corresponding to known states as well as to unidentified states. No sign of the metastable state at about 9.5 eV seen by Wells, Borst, and Zipf could be detected in direct excitation, but an indirect excitation process involving the $A^1\Pi$ state is consistent with the data.

I. INTRODUCTION

Diatomic molecules show pronounced structure in high resolution electron scattering cross section measurements near 10 eV impact energy due to the formation of temporary negative ion states.¹ These shortlived negative ion states, or resonances, are associated with various excited states of the neutral molecule. In CO, a strong resonance at 10.04 eV was first observed in a transmission experiment by Sanche and Schulz,² and shortly afterwards was seen by Comer and Read³ in both the ground state $v=0$ (elastic) and $v=1$ channels. Swanson *et al.*⁴ observed the resonance both in elastic scattering and in its decay to various vibrational levels of the $a^3\Pi$, $A^1\Pi$, and $a'^3\Sigma^+$ states, as did Mazeau *et al.*⁵ shortly afterward. From these measurements, the resonance was identified as a Feshbach or core-excited resonance, with a $1\pi^4 5\sigma 6\sigma^2 2\Sigma^+$ configuration.

Numerous weaker, higher-lying resonances were also observed by Sanche and Schulz.¹ Some of these resonances were also seen by Comer and Read³ in the ground state $v=0$ and $v=1$ channels, and by Mazeau *et al.*⁵ in the $b^3\Sigma^+$ and $B^1\Sigma^+$ channels.

The production of metastables or photons in CO by electron impact near threshold has been measured by several workers, with some controversy in the results. Borst and Zipf⁶ and Wells, Borst and Zipf⁷ have seen evidence of an unidentified metastable state at about 10 eV, which Lawton and Pichanick⁸ have been unable to detect. Newton and Thomas⁹ have seen a peak in uv emission from CO at an incident electron energy of about 8.3 eV, not observed by Wells and Zipf.¹⁰ Ajello¹¹ has measured emission cross sections for vibrational levels of the $a^3\Pi$ and $A^1\Pi$ states from threshold to 300 eV impact energy. Skubenich¹² has done the same up to 100 eV for the $d^3\Delta_i$, $b^3\Sigma^+$, and $B^1\Sigma^+$ electronic states. Mumma, Stone and Zipf¹³ have measured the absolute excitation cross section for the $A^1\Pi$ vibrational levels from threshold to 350 eV impact energy, with results which agree well with those of Ajello.¹¹

To extend our previous measurements⁴ on the resonant structure in CO we have made a series of measurements at incident energies both above and below that of the dominant 10 eV resonance. These measure-

ments were performed at a scattering angle of 45° with the system energy resolution ranging from 13 to 23 meV FWHM, and include observation of resonances in elastic scattering in the 10–12 eV energy region, electron excitation functions of numerous states, and energy loss spectra taken with the incident energy both equal to the resonance energy and swept at a fixed energy above threshold.

II. EXPERIMENTAL

A detailed description of the apparatus has been given previously.¹⁴ Briefly, it consists of a hemispherical electron monochromator-analyzer combination, using a molybdenum cylinder as a static gas target cell. The incident electron beam is monochromatized, adjusted in energy, and focused on the gas cell. The scattered electrons are energy analyzed by the hemispherical analyzer and individually counted by an electron multiplier followed by a fast amplifier and discriminator. The output pulses can be displayed on a count rate meter and X-Y recorder, or counted on a scaler and stored in an on-line computer. The apparatus is normally operated at a resolution of about 40 meV (FWHM of the energy-analyzed elastic scattering peak) at a nominal 10 eV incident electron energy. The resolution as measured in the energy loss mode depends on the resolution of both the monochromator and the analyzer, and the Doppler broadening from the relative motion of the target molecules and the incident electrons. When the instrument is used to measure excitation functions or to observe resonances in elastic scattering the rules for combining these components change. We will therefore state the system resolution applicable to each measurement. The energy is set by a programmable power supply, which is computer-controlled and is accurate to 0.01% of its output ± 0.1 mV.

The CO used in these measurements was 99.8% minimum concentration CO furnished by Matheson. Residual impurities were total hydrocarbons < 250 ppm, $N_2 \approx 73$ ppm and $O_2 \approx 12$ ppm. The CO was admitted to the gas cell through copper and stainless steel tubing using a commercial leak valve to control the gas flow. Typical CO pressures were about 2.7 Pa (20 mTorr) in the gas cell, and about 1000 times less in the surrounding chamber.

One problem in measuring electron excitation functions or energy loss spectra near threshold is the likelihood of energy discrimination in the collection of low energy electrons.¹⁵ An improvement in the collection efficiency for low energy electrons is obtained here by acceleration of the outgoing electrons before they reach a beam-defining aperture, which increases both the effective scattering volume in the gas cell and the angular acceptance of the analyzer for these electrons. This increase in collection efficiency causes a peaking in the transmission of the analyzer near zero energy and may be responsible for the threshold peaks which are present in many but not all of the excitation functions we have measured. The threshold response is sometimes diminished by surface contamination in the scattering cell. Hence we expect, and observe, some variation in the measured intensity in the first 0.4 eV above threshold, when spectra taken weeks apart are compared.

Variations in the collection efficiency and transmission of the analyzer section as a function of scattered electron energy can be eliminated by adjusting the analyzer to accept electrons of only one energy, independent of the incident energy. This mode, called the constant final energy (CFE) mode, is achieved by sweeping both the incident electron energy E_0 and the energy loss E such that the detected scattered electron energy is fixed at $E_0 - E = \text{constant}$. This constant energy difference is the energy above threshold at which each state in the loss spectrum is being excited.

III. RESULTS

A. Resonances in elastic scattering

Figure 1 shows the elastic scattering intensity at 45° in the 10–12 eV energy region measured with a system resolution of 20 meV. The data were accumulated over 4500 computer-controlled sweeps with a total dwell time of 76 sec/point. The energy scale was set by assigning the sharp minimum in the resonance an energy of 10.04 eV. The vertical lines denote the positions of maxima and minima in the derivative of the transmitted current

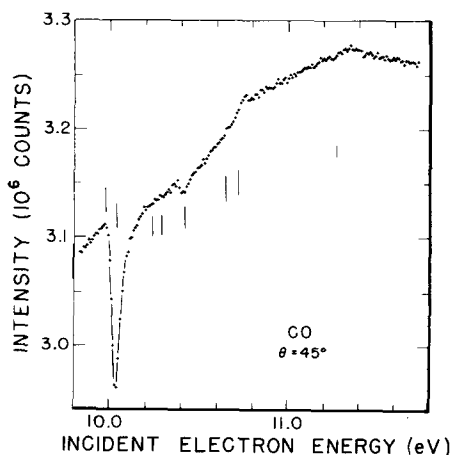


FIG. 1. Elastic scattering intensity for CO at 45° with 20 meV resolution. The vertical lines show the positions of structure seen by Sanche and Schulz (Ref. 1).

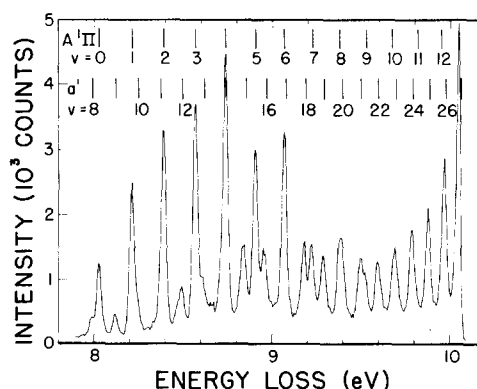


FIG. 2. Energy loss spectrum for CO at 45° with 22 meV resolution measured at the energy of the resonance minimum (10.04 eV). The positions of the $A^1\Pi$ and $a'^3\Sigma^+$ vibrational levels are marked using the energies in Ref. 20.

observed by Sanche and Schulz.¹ We observe a small minimum at 10.42 eV, and sharp steps at 10.65 and 10.77 eV. These structures correspond to the strongest features in Sanche and Schulz's transmission spectrum. The two steps have a height approximately $3\sqrt{N}$, where N is the number of counts, and have been seen in other runs, so we believe them to be real. The general intensity increase with energy is due to electron-optical focusing effects, and is not a real trend in the elastic differential cross section.

The 10.04 eV resonance had an observed width of 43 meV (FWHM) in a run made using a system resolution of 13 meV, in agreement with other measurements.^{3,5} We were also able to observe the decay of the 10.04 eV resonance to the ground state $v=1$ level, obtaining approximately the same shape and intensity relative to the elastic intensity that Comer and Read³ observed at 40° scattering angle in the 9.9 to 10.3 eV region.

B. "On resonance" electron energy loss spectrum

Figure 2 shows an energy loss spectrum from 8–10 eV taken with the incident energy set at the resonance minimum at 10.04 eV. The peaks of the $A^1\Pi$ and $a'^3\Sigma^+$ vibrational series can be seen distinctly, enhanced by the decay of the resonance to the various inelastic channels.¹⁶ The data were taken at 22 meV resolution accumulating 3000 sweeps with a total dwell time of 51 sec/point. The energy scale is believed accurate to about 5 meV. The large peak at the end of the loss spectrum is due to a disproportionately large number of near zero energy electrons being collected by the analyzer as discussed in Sec. II. There may also be some increase in the peak intensities near 10 eV due to higher collection efficiency for very low energy electrons (cf. the gradual rise in the valleys between the peaks from 9.7–10 eV, an effect also seen in the loss spectrum of Mazeau and co-workers⁵).

C. Electron excitation functions below the resonance

Figures 3, 4, and 5 show the electron excitation functions, with the background subtracted, for various vibrational levels of the $a^3\Pi$, $A^1\Pi$, and $a'^3\Sigma^+$ states ob-

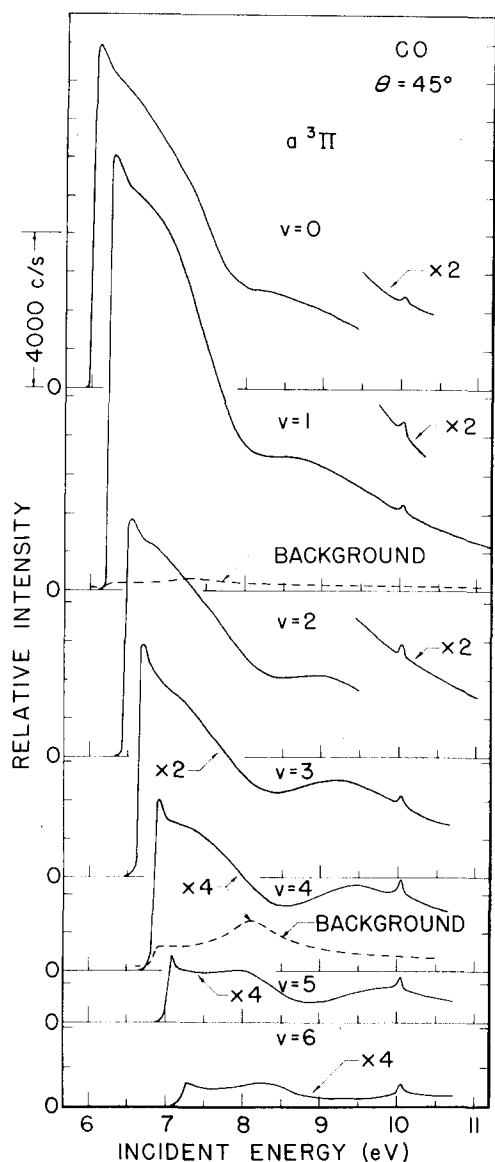


FIG. 3. Excitation functions at 45° of the $a^3\Pi$ vibrational levels taken on an X-Y recorder with 16 meV resolution. A background as shown by the dashed lines has been subtracted from the original traces to give the solid curves. Some of the intensity about 1.3 eV above threshold for the $v=4, 5, 6$, curves may be due to double scattering processes as discussed in the Appendix. The intensity scale has been adjusted to make the relative intensities of Figs. 3, 4 and 5 comparable using the respective count rate scales.

tained on an X-Y recorder in a single sweep using a count rate meter with a two second time constant at system resolutions of 16, 23, and 23 meV FWHM, respectively. The relative intensities of the three figures with respect to each other adjusted for equal resolution are given in terms of count rate on the ordinates, so that the results for the different states may be compared.

The $a^3\Pi$ intensity rises sharply at threshold, then gradually decreases for the lower vibrational levels to a value $\frac{1}{3}$ – $\frac{1}{2}$ that at threshold about 2 eV above threshold. This threshold behavior is also seen in trapped electron spectra, which show very intense $a^3\Pi$ excitation compared to other states for well depths as large

as 0.8 eV or more.^{17,18} Recently, Wong and Schulz¹⁹ have seen resonant structure in ground state vibrational excitation at the energies of the first four $a^3\Pi$ vibrational levels. Our observed threshold enhancement may also be due to this resonance phenomenon.

The background is drawn in as dashed lines in the $v=1$ and $v=4$ spectra, and represents the intensity observed at an energy midway between two peaks. It was subtracted from each vibrational level in turn by lining up background and vibrational thresholds. A peak at 10.04 eV from the decay of the resonance can be seen in the various curves of Fig. 3.

The $v=5$ and $v=6$ levels are considerably weaker in intensity, and hence are more affected by the choice of background level. Also, some of the intensity 1–1.5 eV above threshold may be due to residual tails from double scattering processes. (See Appendix.)

The $A^1\Pi$ excitation functions for $v=0$ –9 are shown

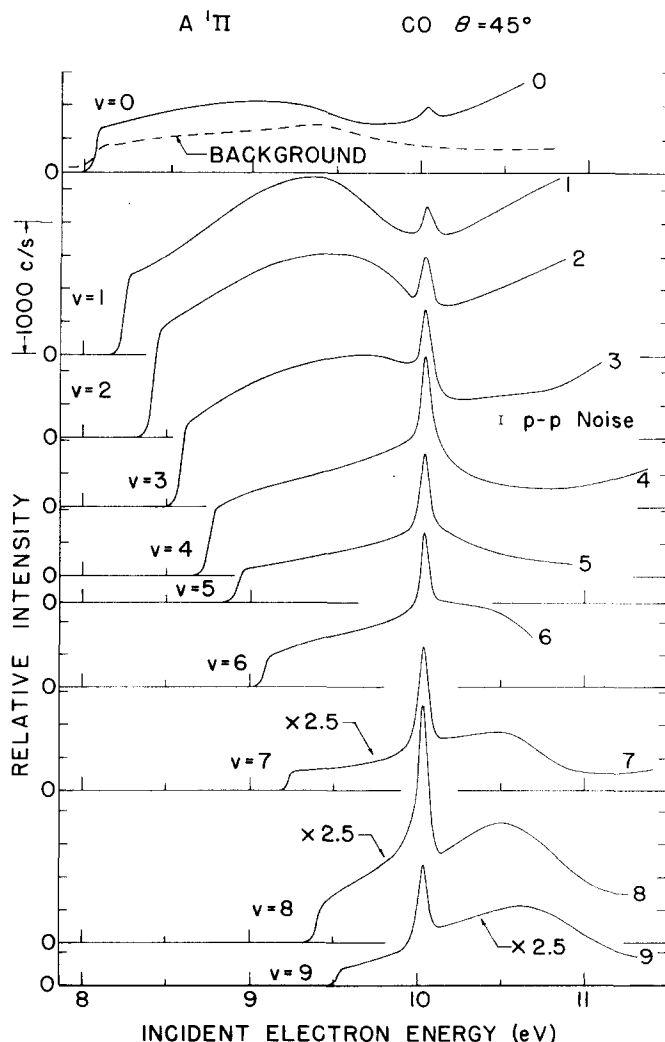


FIG. 4. Excitation functions at 45° of the $A^1\Pi$ vibrational levels taken on an X-Y recorder with 23 meV resolution. A background as shown by the dashed line in $v=0$ has been subtracted from the original traces to give the solid curves. Note the intensity scale change beginning at $v=7$. The peak-to-peak noise in the traces is shown next to $v=4$.

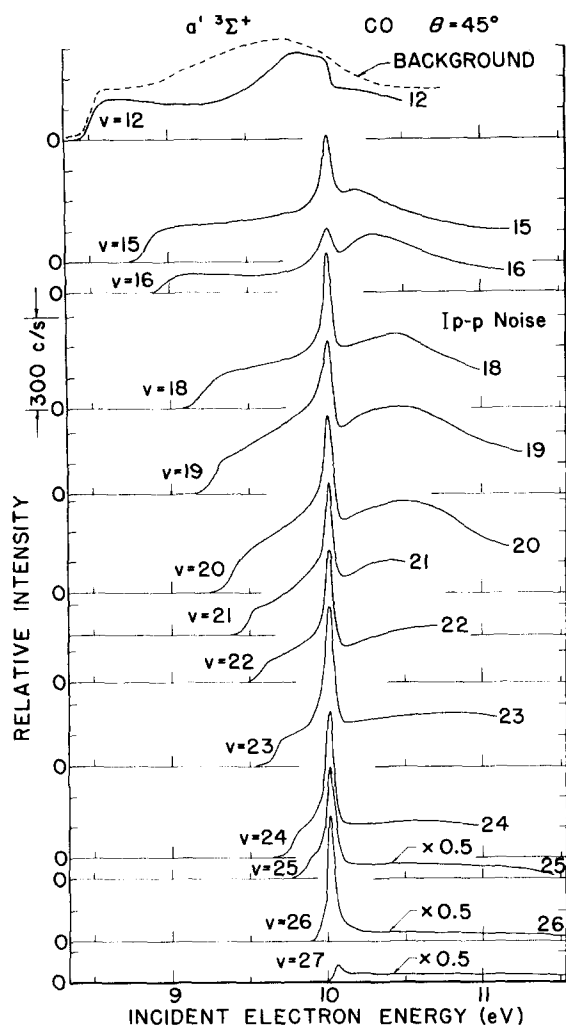


FIG. 5. Excitation functions at 45° of the higher $a'^3\Sigma^+$ vibrational levels taken on an X-Y recorder with 23 meV resolution. A background as shown by the dashed line in $v=12$ has been subtracted as in Figs. 3 and 4. Note the intensity scale change at $v=25$. The peak-to-peak noise in the traces is shown next to $v=18$.

in Fig. 4. These excitation functions show sharp onsets but no peak at threshold, then rise gradually to a broad maximum near the sharp resonance decay peak at 10.04 eV. Above the resonance the intensity begins to increase again.

The intensity of the $v=7$, 8, and 9 excitation functions has been multiplied by 2.5 for display in Fig. 4. The resonance decay peak for $v=8$ appears larger than that for $v=7$ or 9 owing to the overlapping intensity of the $a'^3\Sigma^+ v=20$ level. Similarly the observed $A^1\Pi v=10$, 11, and 12 level intensities are more strongly affected at the resonance energy by resonance decay to neighboring $a'^3\Sigma^+$ levels than by direct decay, as may be seen in Fig. 2.

The background intensity measured at 8.31 eV is shown as a dashed line in the excitation function for $v=0$. The peak to peak noise in the recorder traces is shown next to the $v=4$ excitation function.

Figure 5 shows a series of excitation functions for

the $a'^3\Sigma^+$ state. The dominant feature here is the resonance decay peak in the higher vibrational levels. Note the scale change at $v=25$. From $v=22$ to $v=26$ there is no significant contribution from adjacent states. (See Fig. 2.) However the relative intensities are perturbed by the varying collection efficiency of near-threshold electrons. The $v=27$ level lies just above the resonance, at 10.058 eV, and only the tail of the resonance decay can be seen at threshold. For the levels near 10 eV the nonresonant intensity is extremely weak.

The resonance decay peak for $v=20$ is larger than that for $v=21$ owing to the overlap of the $A^1\Pi v=8$ peak intensity. Similarly the $v=18$ decay peak is increased by overlap with the $A^1\Pi v=7$ level. The excitation functions for $v=13$, 14, and 17 are not shown since they are all strongly affected by more intense neighboring $A^1\Pi$ levels. For $v=12$ and below the effect of the resonance decay diminishes rapidly.

The background is shown as a dashed line in the plot for $v=12$. (The backgrounds subtracted in Figs. 3, 4, and 5 are all of similar shape and intensity.) The peak to peak noise in the recorder traces is shown next to the $v=18$ excitation function.

D. Near-threshold energy loss spectrum

To eliminate the variation of analyzer transmission with electron energy the CFE mode was used with the analyzer set to accept electrons of 0.5 eV energy. At this energy above threshold the excitation functions are slowly varying, yet forbidden states are strongly excited. (See Sec. III.E). The observed spectrum is shown in Fig. 6, with the state assignments of Tilford and Simmons²⁰ below 12 eV and those of Ogawa and Ogawa²¹ above 12 eV. The data were taken in 2000 computer-controlled sweeps with a total dwell time of 34 sec/point at a resolution of about 22 meV. The energy scale is estimated to be accurate to about 5 meV. The data in Fig. 6 were taken in a different mode of operation than the data in Fig. 2, but for order of magnitude comparison there were about twice as many elastically scattered electrons per point in Fig. 6 as in Fig. 2.

There is a prominent unidentified peak at $E=11.265$ eV.²² Tilford and Simmons²⁰ place the $j^3\Sigma^+ v=0$ level at $E=11.281$ eV, about 15 meV too high. Several trapped electron experiments, which measure the threshold excitation probability, show a peak in the 11.25–11.30 eV region.^{17,18} However, neither Skerbele and Lassetre²³ at incident energies of 48 and 23 eV and scattering angles of 12° and 0°, respectively, nor Trajmar *et al.*²⁴ at 20 eV and 20° see a peak there. An excitation function measurement by us at $E=11.26$ eV (Sec. III.E) shows a sharp rise at threshold and gradually decreasing intensity thereafter.

The fact that this unidentified state is excited strongly near threshold but is not observed at higher energies indicates that it is another triplet (or otherwise forbidden) state close to the $j^3\Sigma^+$ state. Tilford and Simmons²⁰ observed a perturbation of the $E^1\Pi$ rotational levels by an unknown state, possibly the $v=1$ level of

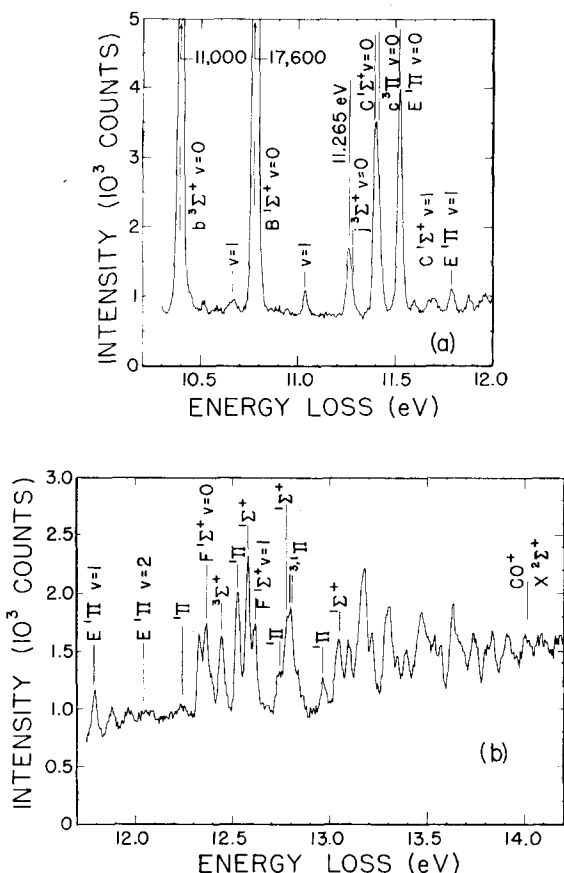


FIG. 6. Energy loss spectrum above the 10.04 eV resonance for CO at 45° with 22 meV resolution, taken by sweeping the incident energy 0.5 eV above threshold (see text). The state assignments of Tilford and Simmons (Ref. 20) and Ogawa and Ogawa (Ref. 21) are noted on the figure.

this unidentified state. (The $j^3\Sigma^+ v=1$ level is too high in energy, at 11.55 eV, to interact with the $E^1\Pi v=0$ level at $E=11.521$ eV.)

The $C^1\Sigma^+$ and $c^3\Pi v=0$ levels appear as one large unresolved peak with a maximum at 11.40 eV. Their respective $v=1$ levels are probably contained in the broad weaker peak centered at 11.69 eV. Unidentified peaks can be seen at 10.51, 11.60, 11.88, 11.96, and 12.33 eV, as well as many others above 13 eV. In analogy with the $C^3\Pi_u$ and $C'^3\Pi_u$ states of N_2 , there may exist a $^3\Pi$ valence state in the 11.5–12.0 eV region which would exhibit a small vibrational interval and could account for the closely spaced, unidentified peaks in this energy range.

E. Electron excitation functions above the 10.04 eV resonance

Excitation functions were measured for several of the prominent states above the resonance. The results are shown in Figs. 7 and 8, and were obtained in 400 computer-controlled sweeps at 20 meV resolution and 7 sec/point dwell time. The intensities of Figs. 7 and 8, when multiplied by 0.5, would be approximately comparable as counts/sec to the data of Figs. 3, 4, and 5. The energy scale was determined by taking the center

of the sharp rise at threshold for each state as the threshold energy, and is believed to be accurate to about 30 meV.

A background run made at $E=11.15$ eV is shown in Fig. 7(e). This background was subtracted from all the excitation functions by shifting the background threshold to coincide in each case with the level threshold and then subtracting a smoothed background intensity from the measured intensity.

Mazeau and co-workers⁵ have measured excitation functions for the parent states of the 10.04 eV resonance, the $b^3\Sigma^+$ and $B^1\Sigma^+$ states. Their $b^3\Sigma^+$ curve for $\theta=40^\circ$ compares well with our curve in Fig. 7(a), the main difference being our very strong threshold peak relative to the 10.7 eV maximum. Our threshold peak is at least partly an instrumental effect, as mentioned earlier. Mazeau *et al.*'s angular distribution data show that the 10.40 eV peak is *s* wave in character, while the 10.7 eV peak has a *p* wave character.

Mazeau *et al.*'s data for the $B^1\Sigma^+ v=0$ state was measured at 60° (not 40° as stated in their figure caption),²⁵ so their result is not directly comparable with ours.

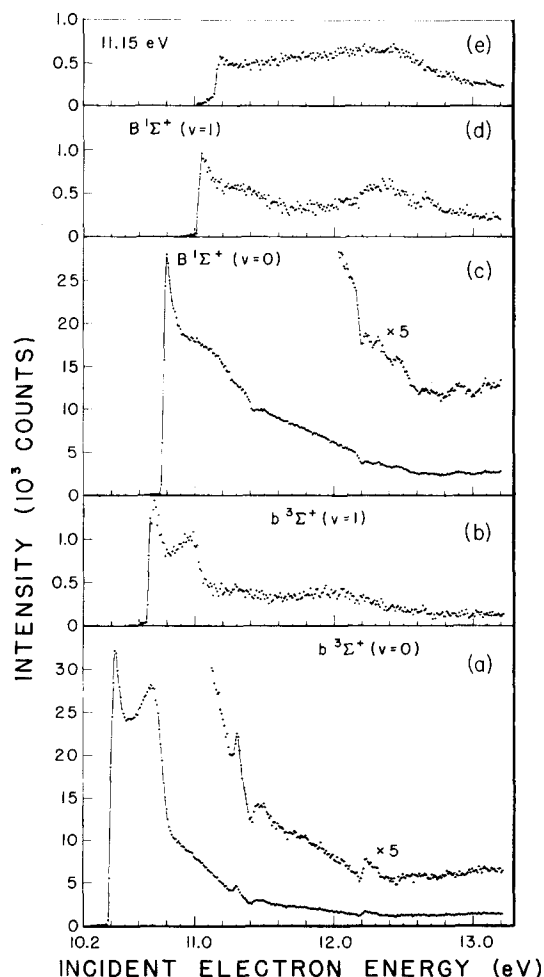


FIG. 7. Excitation functions at 45° with the background subtracted for various states above the resonance at 20 meV resolution. (a) $b^3\Sigma^+ (v=0)$, $E=10.394$ eV; (b) $b^3\Sigma^+ (v=1)$, $E=10.665$ eV; (c) $B^1\Sigma^+ (v=0)$, $E=10.776$ eV; (d) $B^1\Sigma^+ (v=1)$, $E=11.034$ eV; (e) background, $E=11.15$ eV.

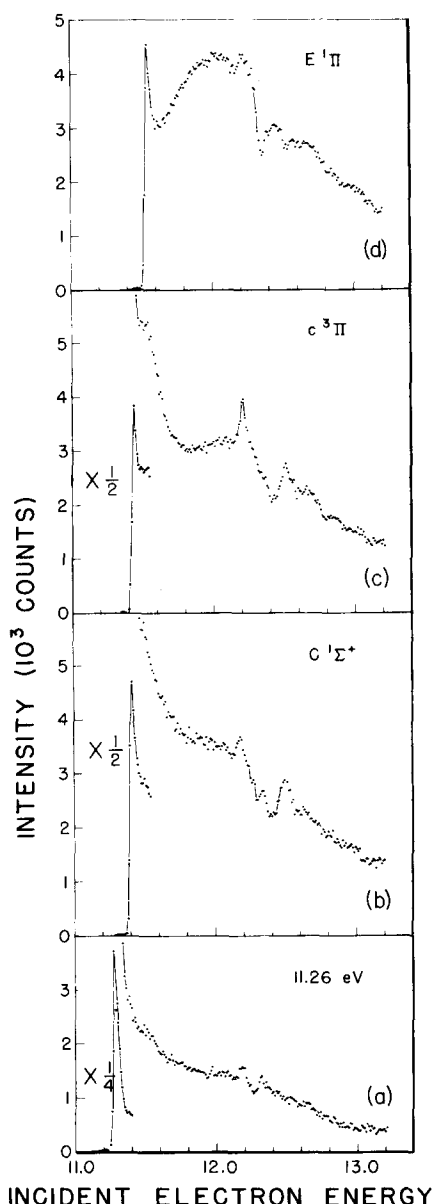


FIG. 8. Excitation functions at 45° with the background subtracted for various states above the resonance at 20 meV resolution (a) $E=11.26$ eV; (b) $C^1\Sigma^+$ ($v=0$), $E=11.396$ eV; (c) $c^3\Pi$ ($v=0$), $E=11.416$ eV; (d) $E^1\Pi$ ($v=0$), $E=11.521$ eV. The ordinates of Figs. 7 and 8 can be compared to determine relative intensities between the two figures.

We see (beyond the sharp threshold peak) resonant structure at 11.25–11.4 eV and 12.2 eV, plus a general lumpiness beyond 12.2 eV.

The $b^3\Sigma^+$ ($v=1$) excitation function shows a peak at 11.0 eV similar to the 10.7 eV peak in the $v=0$ level (the small change in slope for $v=0$ at 11.0 eV is spurious, not observed in other runs). The broad peaks in the $b^3\Sigma^+$ ($v=1$) and $B^1\Sigma^+$ ($v=1$) excitation functions at about 12.0 and 12.4 eV, respectively, are probably due to residual background intensity.

Figure 8(a) shows the excitation function for the state at 11.26 eV described in Sec. III. D. The intensity within 0.15 eV of threshold has been multiplied by 0.25

for display purposes. The excitation function at $E=11.281$ eV corresponding to the $j^3\Sigma^+$ state was also measured, but appeared to consist primarily of the intensity associated with the wing of the 11.26 eV peak. The weak peak at about 11.5 eV is real, while the four point "staircase" at 11.95 eV is not.

The $C^1\Sigma^+$ ($v=0$) and $c^3\Pi$ ($v=0$) states at 11.396 and 11.416 eV, respectively, could not be resolved, and the excitation function of each contains a large contribution from the other. However, qualitatively they seem to be of comparable intensity (cf. Fig. 6) at least near threshold. The $c^3\Pi$ excitation function intensity decreases to a minimum beyond threshold before rising to the resonant peak at 12.2 eV, while the $C^1\Sigma^+$ intensity shows a gradual decrease from the threshold peak to the 12.2 eV peak. The $C^1\Sigma^+$ intensity also has a subsidiary maximum at 12.34 eV not visible in the $c^3\Pi$ excitation function. The three higher levels in Fig. 8 show pronounced structure in the 12.15–12.6 eV region corresponding to the lumpiness in the $B^1\Sigma^+$ ($v=0$) excitation function above 12.2 eV.

At higher energies, the $F^1\Sigma^+$ state (not shown in Fig. 8) at $E=12.365$ eV has a peak at threshold as well as a subsidiary maximum at $E=12.55$ eV. The excitation function for $E=13.17$ eV also shows a marked threshold peak.

In numerous cases in our data a new inelastic channel opens with (possibly) associated resonant structure appearing in lower energy inelastic channels.

IV. DISCUSSION

Since we now have a rather complete picture of the excitation of CO by low energy electrons, we can analyze the results of several experiments which measure the production of photons or metastables in CO by electron impact.

Mumma, Stone, and Zipf¹³ measured the absolute optical excitation cross sections for the $A^1\Pi$ ($v=0-5$) bands from the emission spectrum of the fourth positive system ($A^1\Pi-X^1\Sigma^+$). Their results are in good agreement with those of Ajello,¹¹ who measured the $A^1\Pi$ ($v=0$)– $X^1\Sigma^+$ ($v=1$) band intensity and estimated its contribution to the total emission intensity. Both results show the excitation cross section rising from threshold to a maximum at 23 eV and then decreasing gradually. Our electron excitation function measurement for the $A^1\Pi$ ($v=2$) level shows a gradual increase in intensity above the 10 eV resonance to a broad maximum near 20 eV before decreasing again at higher energies, in qualitative agreement with the optical measurements.

Ajello¹¹ also measured the emission cross section for the Cameron system ($a^3\Pi-X^1\Sigma^+$) from threshold to 300 eV. For the Cameron band system (integrated over vibrational levels), Ajello obtained a maximum emission cross section of 1.1×10^{-18} cm² ($\pm 75\%$) at $E_0=11$ eV assuming ≈ 1 msec lifetime for the $a^3\Pi$ state as determined by Borst and Zipf.⁶ Cascading from the $d^3\Delta_1$ and $b^3\Sigma^+$ levels was considered to be small, based on measurements by Skubenich¹² on the triplet bands ($d^3\Delta_1-a^3\Pi$) and third positive system ($b^3\Sigma^+-a^3\Pi$) which

show peak emission cross sections near threshold of roughly $5 \times 10^{-18} \text{ cm}^2$ and $2 \times 10^{-18} \text{ cm}^2$ respectively. The cascade contribution of the Asundi bands ($a'^3\Sigma^+ \rightarrow a^3\Pi$) is not known.

More recent measurements^{26,27} on the $a^3\Pi$ lifetime show good agreement with a theoretical calculation of James²⁸ and indicate a mean lifetime of about 9 ± 1 msec. Since Ajello's cross section value depends linearly on the lifetime,²⁹ his cross section should be scaled upward a factor of 9, to $\approx 1.0 \times 10^{-15} \text{ cm}^2$. This result is "unreasonably large" to quote Wells *et al.*,²⁹ particularly when compared to an angular distribution measurement of Trajmar²⁴ for 20 eV electrons scattered from CO. Trajmar's results would indicate a total cross section for $a^3\Pi$ excitation of approximately $3 \times 10^{-17} \text{ cm}^2$, only 10% of Ajello's (scaled) result at 20 eV. Also, our electron excitation function measurement for the $a^3\Pi$ ($v=1$) level at 45° shows a continuous monotonic decrease in intensity from the threshold maximum out to $E_0 = 24$ eV, and several trapped electron measurements^{17,18} even at well depths as low as 50 meV indicate a very large $a^3\Pi$ excitation cross section at threshold, rather than the gradually increasing cross section shown in Fig. 8 of Ajello.¹¹

The fact that Ajello observes the maximum emission cross section near 11 eV impact energy,³⁰ while our measurements and the trapped electron results show the maximum cross section for $a^3\Pi$ excitation to be near threshold, is evidence that significant cascading from higher states occurs. Such cascading could come from the $b^3\Sigma^+$ state, which we observe to be strongly excited near 11 eV, and from which an optically allowed transition can be made to the $a^3\Pi$ levels. Higher triplet states may also contribute.

Controversy has recently arisen concerning the existence of a new metastable state in CO. In their measurement of the $a^3\Pi$ lifetime, Borst and Zipf⁶ observed another, shorter-lived, metastable state with a threshold energy of about 10 eV. Cermak³¹ and Olmsted *et al.*³² also have seen evidence for a metastable state (or states) in CO of energy ≈ 10 eV. Later, Wells, Borst, and Zipf⁷ located this state at 9.5 ± 0.4 eV and determined its lifetime to be 97 ± 15 μsec , much less than that of the $a^3\Pi$ state. The peak cross section for excitation of this unidentified metastable state was estimated to be $3 \times 10^{-18} \text{ cm}^2$ at 15 eV. Since the $b^3\Sigma^+$ lifetime is about 60 nsec, they rejected this assignment and suggested the $D^1\Delta$ or $I^1\Sigma^-$ states as possibilities.

However, energy loss spectra of CO taken at low incident energies show no indication of such states in the 6–11 eV energy region with any appreciable excitation cross section.^{4,17,18,23} In particular, Fig. 8 of Wells *et al.*⁷ shows a total excitation cross section for this state larger than that of the $b^3\Sigma^+$ state¹² at 12 and 20 eV, but an energy loss spectrum at 45° taken by us at 12.2 eV with 45 meV resolution shows no peak greater than 5% of the $b^3\Sigma^+$ peak height attributable to such a state in the 9–11 eV region. Trajmar,²⁴ in an angular distribution measurement of 20 eV electrons scattered in CO, also sees no sign of any of these states in this region. In Fig. 2 every loss peak can be as-

signed to either the $a'^3\Sigma^+$ or $A^1\Pi$ states. Thus the direct excitation of this new metastable state is not supported. More probably the excitation process is the strong excitation of the $A^1\Pi$ state followed by decay both to the ground state and to the $D^1\Delta$ and $I^1\Sigma^-$ metastable states.³³ The intermediate $A^1\Pi$ state provides the coupling between the ground state and the metastable states by becoming excited in a transition to the left side of its internuclear potential well and decaying from the right side, thus circumventing the low transition probability of the direct process.

The existence of a resonance in the 8 to 9 eV region, causing enhanced excitation of the $a'^3\Sigma^+$ state, has been suggested by Newton and Thomas.⁹ They measured the prompt uv photon emission from CO in the 6–15 eV impact energy range, and observed a broad peak at an electron energy of 8.3 eV, with an onset at about 7.4 eV. This peak, if real, must be due to decay to the ground state, since the lowest excited state is the $a^3\Pi$ at 6.0 eV. Newton and Thomas suggested the possibility of population of $a'^3\Sigma^+$ levels by a resonance mechanism in the 8 eV region and subsequent decay to the ground state. Wells and Zipf¹⁰ repeated these measurements using a similar experimental arrangement and saw no peak at all near 8 eV, although agreement between the two experiments was good in the 11–15 eV region. In our excitation functions for the $a'^3\Sigma^+$ levels with thresholds above 8.3 eV, no sign of resonant structure can be seen in the 8.5–9 eV region (see Fig. 5, particularly $v=12$).

From the preceding discussion we see that electron spectroscopy, where the energy of the state being excited is unambiguously known, is a powerful technique for studying the electron excitation of molecules. It may therefore extend, confirm or refute the conclusions drawn from the results of less direct techniques.

ACKNOWLEDGMENT

We would like to thank Dr. Morris Krauss for numerous discussions and suggestions on the interpretation of the data.

APPENDIX

In excitation functions measured with poorer system resolutions (≥ 25 meV FWHM), the $a^3\Pi$ $v=4, 5$, and 6 levels showed a broad rise in intensity about 1–1.3 eV above threshold. To study this effect in more detail, the CFE mode was used, with the analyzer set for an outgoing electron energy of 1.2 eV. One such spectrum obtained at a resolution of 22 meV is shown in Fig. 9. Additional peaks, not due to $a^3\Pi$ or $a'^3\Sigma^+$ vibrational excitation, can be seen at 6.27, 6.49, 6.54, 6.70, 6.75, 6.90, and 6.96 eV. We attribute these peaks to double scattering processes involving an $a^3\Pi$ vibrational excitation followed by a resonant ground state vibrational excitation.

Ehrhardt *et al.*³⁴ have measured cross sections for excitation of the various ground state vibrational levels in the 0–4 eV energy range, and found very strong enhancement of the $v=1-3$ excitation cross section for in-

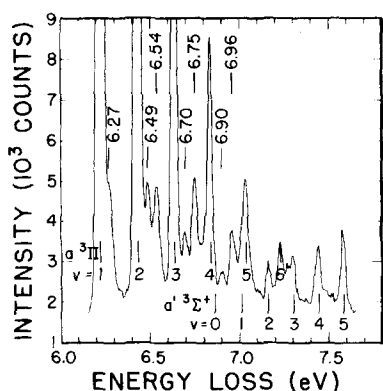


FIG. 9. Energy loss spectrum for CO at 45° with 22 meV resolution, taken by sweeping the incident energy 1.2 eV above threshold (see text). Additional peaks can be seen (labelled by their energy loss values) due to double scattering processes, viz., an $a^3\Pi$ excitation followed by a resonant ground state vibrational excitation. The zero level is suppressed one vertical division.

cident energies from 1.4–2.4 eV. The 6.27, 6.49, 6.70, and 6.90 eV loss peaks are thus believed to result, respectively, from an $a^3\Pi$ $v=0, 1, 2$, and 3 excitation, followed by a resonant excitation of the $X^1\Sigma^+$ $v=1$ level (excitation energy 0.27 eV) at 1.47 eV to yield the detected electron of 1.2 eV energy. Similarly the 6.54, 6.75, 6.96, and 7.16 eV loss peaks (the latter merged with the $a'^3\Sigma^+$ $v=2$ peak) result from $a^3\Pi$ excitation ($v=0-3$) followed by a resonant excitation of the $X^1\Sigma^+$ $v=2$ level (excitation energy 0.53 eV).

There is no indication of an $a^3\Pi$ $v=0$ or 1 excitation combined with an $X^1\Sigma^+$ $v=3$ excitation (0.79 eV) to give peaks at 6.80 or 7.01 eV, presumably because at 1.99 eV the cross section for ground state $v=3$ excitation is much less than that for $v=1$ excitation at 1.47 eV.³⁴

The intensity of each of the second series of peaks (6.54 eV, *et seq.*) is roughly comparable to that of the corresponding peak of the first series (6.27 eV, *et seq.*), in disagreement with the results of Ehrhardt *et al.*,³⁴ who measured the excitation cross section for the $X^1\Sigma^+$ $v=1$ level at 1.47 eV to be about three times that of the $v=2$ level at 1.73 eV. (The decrease in intensity of the $a^3\Pi$ excitation functions between 1.47 and 1.73 eV above threshold is not sufficient to account for the discrepancy.) However, the relative intensities of the peaks within a series follow closely their respective $a^3\Pi$ vibrational intensities 1.5–1.7 eV above threshold.

In data taken with larger half-widths the tails of these double scattering peaks are sufficiently large in the vicinity of the $v=4, 5$, and 6 peaks compared to the peaks themselves to give significant intensity in the excitation functions 1–1.5 eV above threshold. The combination of very high excitation probability 1.5 eV or so from threshold for the first few $a^3\Pi$ levels as compared to the low excitation probability 1–1.5 eV above threshold for the $v=4, 5$, and 6 levels (see Fig. 3), and the large resonant ground state vibrational excitation cross section beginning at about 1.4 eV make the double scattering process unusually visible in this case.

Since the $A^1\Pi$ and $a'^3\Sigma^+$ excitation functions are considerably weaker in intensity 1.5 eV or so above threshold than the first few $a^3\Pi$ levels, the double scattering process is much less likely to occur in these measurements. Also, the $A^1\Pi$ intensities 1.5 eV above threshold are not large compared to the intensities of nearby higher-lying $A^1\Pi$ levels in the 1–1.5 eV region above threshold, so that the contribution of double scattering processes to the $A^1\Pi$ results is probably negligible. The higher $a'^3\Sigma^+$ levels are sufficiently low in intensity, however, that some contribution from $A^1\Pi$ plus resonant ground state vibrational excitation to some of the $a'^3\Sigma^+$ data cannot be ruled out.

- ¹L. Sanche and G. J. Schulz, Phys. Rev. A 6, 69 (1972).
- ²L. Sanche and G. J. Schulz, Phys. Rev. Lett. 26, 943 (1971).
- ³J. Comer and F. H. Read, J. Phys. B 4, 1678 (1971).
- ⁴N. Swanson, C. E. Kuyatt, J. W. Cooper, and M. Krauss, Phys. Rev. Lett. 28, 948 (1972).
- ⁵J. Mazeau, F. Gresteau, G. Joyez, J. Reinhardt, and R. I. Hall, J. Phys. B 5, 1890 (1972).
- ⁶W. L. Borst and E. C. Zipf, Phys. Rev. A 3, 979 (1971).
- ⁷W. C. Wells, W. L. Borst, and E. C. Zipf, Phys. Rev. A 8, 2463 (1973).
- ⁸S. A. Lawton and F. M. J. Pichanick, Abstracts IIIrd International Conference on Atomic Physics, Boulder, CO, 1972, p. 145.
- ⁹A. S. Newton and G. E. Thomas, Chem. Phys. Lett. 11, 171 (1971).
- ¹⁰W. C. Wells and E. C. Zipf, J. Chem. Phys. 57, 3583 (1972).
- ¹¹J. M. Ajello, J. Chem. Phys. 55, 3158 (1971).
- ¹²V. V. Skubenich, Opt. Spectrosc. 23, 540 (1967).
- ¹³M. J. Mumma, E. J. Stone, and E. C. Zipf, J. Chem. Phys. 54, 2627 (1971).
- ¹⁴N. Swanson, J. W. Cooper, and C. E. Kuyatt, Phys. Rev. A 8, 1825 (1973).
- ¹⁵G. J. Schulz, Rev. Mod. Phys. 45, 423 (1973).
- ¹⁶In Ref. 4 we displayed both the "on" and "off" resonance energy loss spectra at 45° at about 40 meV resolution and estimated the enhancement in the various levels from the resonance decay.
- ¹⁷H. H. Brongersma, A. J. H. Boerboom, and J. Kistemaker, Physica (Utr.) 44, 449 (1969); C. E. Brion and L. A. R. Olsen, J. Chem. Phys. 52, 2163 (1970); Chem. Phys. Lett. 15, 442 (1972).
- ¹⁸J. Reinhardt, G. Joyez, J. Mazeau, and R. I. Hall, J. Phys. B 5, 1884 (1972).
- ¹⁹S. F. Wong and G. J. Schulz, Phys. Rev. Lett. 33, 134 (1974).
- ²⁰S. G. Tilford and J. D. Simmons, J. Phys. Chem. Ref. Data 1, 147 (1972).
- ²¹S. Ogawa and M. Ogawa, J. Mol. Spectrosc. 49, 454 (1974).
- ²²This peak is not due to the $E_0^1\Sigma^+$ state mentioned in Krupenie's critical review article [P. H. Krupenie, Natl. Stand. Ref. Data Ser. 5 (1966)]. The existence of the $E_0^1\Sigma^+$ state was based on an emission spectrum of CO now believed to have been contaminated by N_2 [J. D. Simmons (private communication)] and was not seen by Tilford and Simmons (Ref. 20). The electron scattering data involves excitation from the ground state (i.e., as in optical absorption), so we would not see N_2 contamination at that energy.
- ²³A. Skerbele and E. N. Lassettre, J. Chem. Phys. 55, 424 (1971).
- ²⁴S. Trajmar, W. Williams, and D. C. Cartwright, Abstracts VII ICPEAC, (North-Holland, Amsterdam, 1971), p. 1066.
- ²⁵J. Mazeau (private communication).
- ²⁶C. E. Johnson and R. S. Van Dyck, Jr., J. Chem. Phys. 56, 1506 (1972).

- ²⁷G. M. Lawrence, Chem. Phys. Lett. 9, 575 (1971) and references in Table I.
- ²⁸T. C. James, J. Chem. Phys. 55, 4118 (1971).
- ²⁹W. C. Wells, W. L. Borst, and E. C. Zipf, J. Geophys. Res. 77, 69 (1972).
- ³⁰The reason for the good agreement of Ajello's $A^1\Pi$ cross section with Mumma, Stone and Zipf (Ref. 13), combined with the exceptionally large value of his $a^3\Pi$ cross section probably originates in Ajello's treatment of the decay of the $a^3\Pi$ state in his spectrometer, as well as in any contribution from cascade.
- ³¹V. Cermak, J. Chem. Phys. 44, 1318 (1966).
- ³²J. Olmsted III, A. S. Newton, and K. Street, Jr., J. Chem. Phys. 42, 2321 (1965).
- ³³The two step excitation process was suggested to us by R. Freund (private communication).
- ³⁴H. Ehrhardt, L. Langhans, F. Linder, and H. S. Taylor, Phys. Rev. 173, 222 (1968).